

Power Efficient Simultaneous Wireless Information Transception and Power Reception Through an Isolation Barrier

Lukas Hüssen¹, Muh-Dey Wei, Renato Negra

Chair of High Frequency Electronics, RWTH Aachen University, Germany

¹Lukas.Huessen@HFE.RWTH-Aachen.de

Abstract—We present a power efficient structure for simultaneous wireless information transception and power reception through an isolation barrier. The structure utilises a binary frequency shift keying (BFSK) communication scheme for efficient power and information reception and on-off-keying (OOK) harmonic backscattering for information transmission. The structure achieves an overall system efficiency above 55 % from 20 dBm to 26 dBm input power while receiving a BFSK signal with up to 40 MSym and backscattering a 100 kHz PWM signal.

Keywords—backscattering, bidirectional communication, near field coupling, simultaneous wireless information and power transfer (SWIPT), wireless power transfer

I. INTRODUCTION

In high voltage circuits certain parts need to be galvanically isolated. Signals as well as power need to be exchanged across such galvanic isolation barriers. Traditionally, opto-electronics and magnetic cores are the key enablers of isolated signal and power transfer, respectively. A power of more than 1 W can be transferred with above 52 % efficiency using magnetic cores in a fully integrated chip [1]. To transfer power and signals, other types of couplers have been explored, *e.g.* a piezoelectric transformer [2]. In this paper, we propose the use of a simultaneous wireless power and information transfer (SWIPT) system, in combination with harmonic backscattering, for simultaneous wireless information transception and power reception through an isolation barrier.

Harmonic reflection tags use a nonlinear element to generate the second harmonic of a signal coming from a transmitter and emit this harmonic signal to be detected [3], [4]. In harmonic backscattering this harmonic signal is modulated such that backward communication is possible. This technique finds its most common application in RFID systems [5]. It has been further developed to enable simultaneous backscattering and the reception of an incoming modulated signal in a communication tag [6]. A 915 MHz receiver, which is able to switch between power harvesting and harmonic backscattering, has been implemented [7], enabling battery-free operation. Battery-free operation has been demonstrated in [8] by utilising the power from an incoming 915 MHz signal to supply a communication transceiver operating at 2.4 GHz. Operating power reception and backscatter communication at different, but close, frequencies in the GHz range has also been explored [9], [10]. In [11] and [12] a diode rectifier was used for power harvesting and the generated second harmonic was utilised

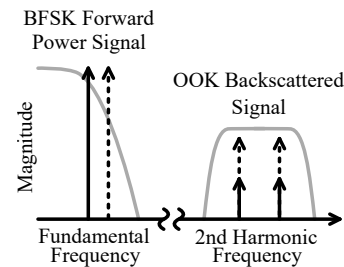


Fig. 1. Modulation frequency spectrum

for on-off-keying (OOK) harmonic backscatter communication modulated by a PIN-diode based band-stop filter and a capacitance based harmonic termination, respectively.

In this work, harmonic backscattering of an OOK signal combined with a BFSK-signal for wireless power reception by a diode-based rectifier is demonstrated for simultaneous wireless information transception and power reception through an isolation barrier. The system reaches above 55 % overall efficiency from 20 dBm to 26 dBm input power, and a peak measured output power of 24.6 dBm at 27 dBm input power. Both the demodulation of the forward BFSK and the backward OOK signals are demonstrated.

II. SYSTEM DESIGN

Fig. 1 and Fig. 2 show the utilised frequency spectrum and a photograph of the system. The BFSK forward signal used for SWIPT switches between 2.4 GHz and 2.41 GHz and can be demodulated by a low-pass filter. The power of the transmitted BFSK signal can be recovered by a rectifier. The backscattered OOK signal will be at 4.8 GHz and 4.82 GHz and modulated in amplitude, it can be filtered by a band-pass and demodulated by a 4.8 GHz power detector on the transmission side as shown in Fig. 2.

For prototyping, the system was deliberately split up in multiple components, *i.e.* dualband coupler, power rectifier, backscatter switch, filters, and power detectors, to verify their functionality individually. Each component was implemented on a Rogers 4350b substrate with 0.762 mm thickness. The dualband coupler is a capacitive near-field coupler which has a measured coupling loss of 0.239 dB at 2.4 GHz. This provides galvanic isolation by the thickness of the substrate and should, considering the dielectric strength $DS = 31.2 \text{ kV/mm}$, given in the substrate datasheet, hold up to an isolation voltage of 23 kV.

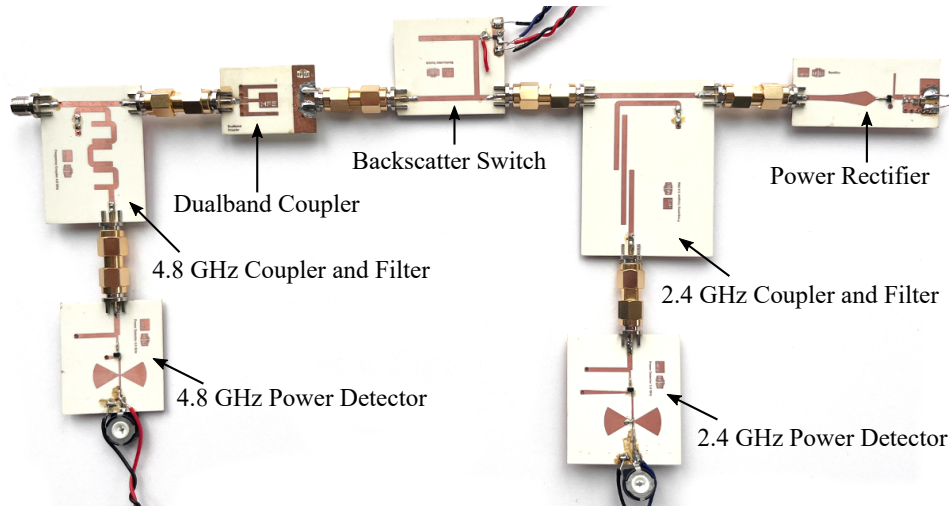


Fig. 2. System overview.

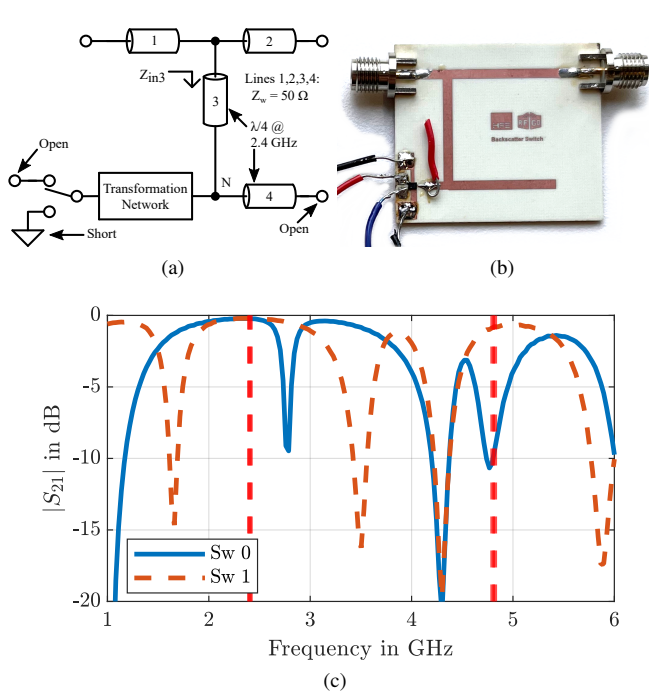


Fig. 3. Designed backscatter switch: (a) schematic, (b) photograph, and (c) measured transfer characteristic, S_{21} .

The power rectifier utilises two Infineon BAT68 diodes in voltage doubler configuration. It provides a maximum measured power efficiency of 79% at 2.4 GHz and 23 dBm input power.

Both 2.4 GHz and 4.8 GHz power detectors are implemented using the Infineon BAT15 diodes. They are each loaded with a 5 k Ω potentiometer. On the transmitter side, to filter the backscattered signal, without affecting the forward signal, a 10 dB-coupler is combined with a hairpin filter. The forward path exhibits 0.28 dB measured loss at 2.4 GHz, while the backscattered signal is coupled with

–20.35 dB to the input of the power detector at 4.8 GHz. On the receiver side side, to filter the forward signal, a 20 dB-coupler is combined with a coupled line bandpass filter. The backscattered signal travels through with 0.57 dB measured attenuation and the forward signal with 0.24 dB attenuation. A part of the forward signal is coupled to the power detector with 24.1 dB measured attenuation at 2.4 GHz and 25.25 dB attenuation at 2.41 GHz.

Due to the low percentage of power coupled to the power detectors, the overall path loss from input to the power rectifier is equal to only 1 dB, with 0.24 dB added from the backscatter switch. This means 79% of the power entering the system is forwarded to the power rectifier. Taking the rectifier efficiency of 79% into account this gives a maximum system efficiency of 62%, which is closely confirmed in measurements.

Fig. 3 shows the schematic of the backscatter switch, a closeup of the PCB and its measured transfer characteristic. Z_{in3} determines the attenuation of the second harmonic, while keeping the attenuation at the fundamental constant. Both line 3 and 4 are designed to have an electric length of $\lambda/4$ at 2.4 GHz. The open stub, line 4, creates a short at node N at the fundamental frequency leading to open/high impedance at Z_{in3} as well as independence of the transformation networks input impedance. Thus, the fundamental frequency and the second harmonic are decoupled.

At the second harmonic, line 3 and line 4 turn to $\lambda/2$ electric length, wherefore Z_{in3} is equal to the input impedance of the transformation network. The input impedance of the transformation network can be switched between two states using an RF-switch, a low-cost BGS12PN10 from Infineon, which connects either to an open or a short circuit. At the fundamental frequency, the attenuation is 0.24 dB at state 0 and 0.22 dB at state 1, which gives low losses and nearly no difference between the states. At the second harmonic, however, the attenuation is 10.3 dB at state 0 and 0.87 dB at state 1, enabling the amplitude modulation of the harmonic.

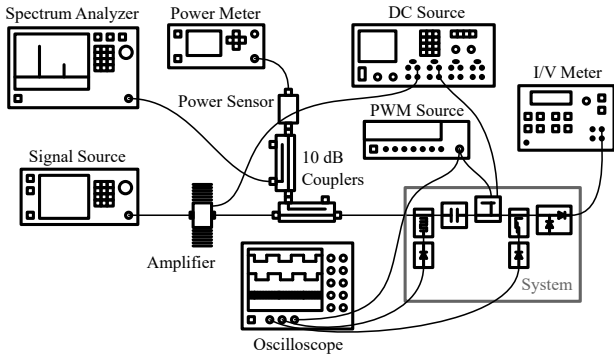
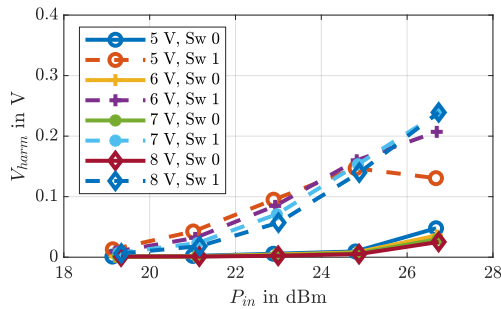
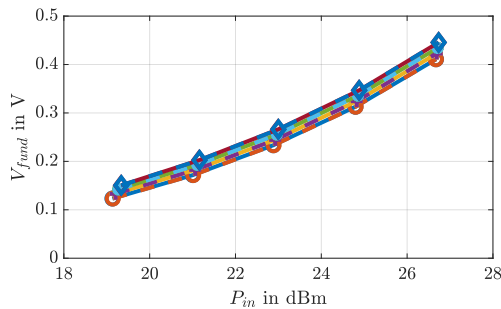


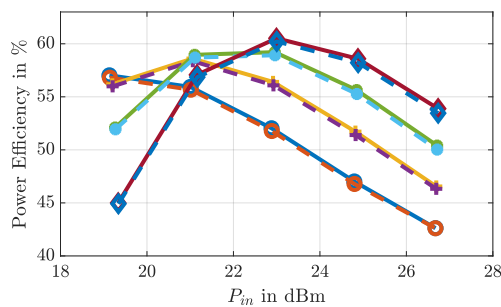
Fig. 4. Measurement setup.



(a)



(b)

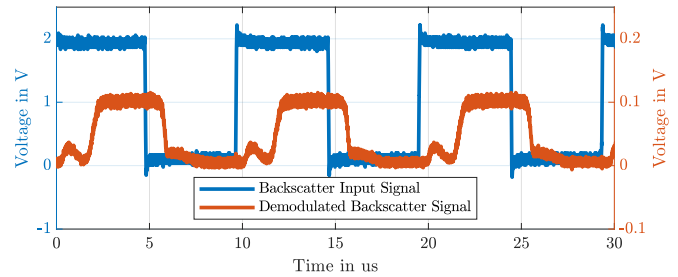


(c)

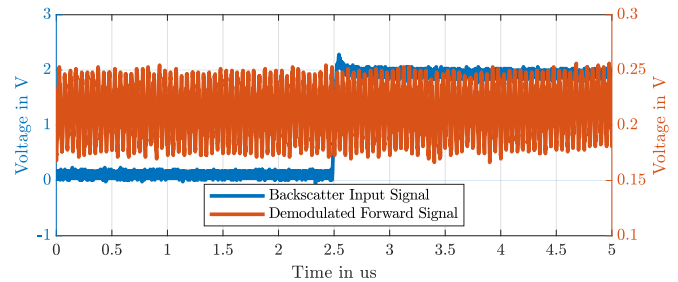
Fig. 5. Measured voltage response of (a) the harmonic and (b) fundamental detector at the two backscatter switch states and (c) overall system power efficiency.

III. MEASUREMENTS

The measurement setup used to characterise the full system is shown in Fig. 4. The input signal was enhanced by an amplifier and its spectrum and power measured via



(a)



(b)

Fig. 6. Measured time-domain waveform: (a) demodulated backscatter signal and (b) demodulated forward signal at 40 MSym forward signal together with 100 kHz backscatter PWM at 25 dBm input power.

10 dB directional couplers. The output of the rectifier was connected to a I/V meter which set the voltage and measured the current to get the output power. The detector outputs and the backscattering input signal were measured using an oscilloscope.

In Fig. 5 the voltage response and the efficiency of the system at various output voltages and the two switching states are shown. The voltage response of the harmonic power detector in Fig. 5a shows a clear difference between the two switching states, which are resembled by the dashed and solid line. The output voltage does not have much influence on the behaviour, only when high input power is combined with a low output voltage, at which point the reflected harmonic power of the rectifier deteriorates. The voltage response of the fundamental detector in Fig. 5b shows that the backscatter switch works as intended, as the lines of both switching states are nearly congruent. Also, the output voltage does not influence the measurement much, which is desired. The overall system power efficiency in Fig. 5c peaks at 23 dBm input power and 8 V output voltage above 60%. It is shown that, using the output voltage, it can be kept above 55% from 20 dBm to 26 dBm input power. Furthermore, the switching state has nearly no influence on the system efficiency with a maximum of 0.43% difference at the highest power and output voltage state.

To demonstrate the data performance, a BFSK forward signal and a PWM backscatter signal were applied to the system, simultaneously. The time domain signals are shown in Fig. 6. The backscatter signal is a 100 kHz PWM, of which the maximum frequency is solely limited by the RF-switch used in the backscatter switch. The forward signal of 40 MSym can be demodulated and is not influenced by the backscattered signal.

IV. CONCLUSION AND OUTLOOK

We proposed and demonstrated a system to power efficiently simultaneously transept wireless information and receipt power through an isolation barrier. The system utilises a BFSK scheme for power and information reception and harmonic backscattering for information transmission. A backscatter switch is demonstrated that has nearly no influence on the system at the fundamental frequency, but efficiently modulates the power at the second harmonic for backscattering communication. A system power efficiency above 55 % from 20 dBm to 26 dBm input power was measured and the signal integrity up to 40 MSym forward and 100 kHz PWM backward was demonstrated in this prototype. An even higher efficiency can be expected in a single-PCB implementation due to the absence of connector losses and increased compactness. A series of applications using this system is anticipated and will be demonstrated in the future.

ACKNOWLEDGMENT

This work was supported by the Federal Ministry of Education and Research (BMBF) under the grant number 16KISK171.

REFERENCES

- [1] Z. Yue, M. Shaoyu, Z. Tianting, Q. Wenhui, Z. Yuanyuan, G. Yingjie, and C. Baoxing, "A 52% Peak-Efficiency >1W Isolated Power Transfer System Using Fully Integrated Magnetic-Core Transformer," in *IEEE Solid-State Circuits Conf.*, Feb. 2019, pp. 244–246, doi: 10.1109/ISSCC.2019.8662301.
- [2] P. Valenta, V. Koucký, and J. Hammerbauer, "Simultaneous power transfer and information transfer via piezoelectric transformer," in *Telecommun. Forum*, Nov. 2017, doi: 10.1109/TELFOR.2017.8249412.
- [3] K. Gumber, F. Amato, C. Dejous, and S. Hemour, "Nonlinear Negative Resistance-based Harmonic Backscatter," in *Int. Microw. Symp.*, Aug. 2020, pp. 603–606, doi: 10.1109/IMS30576.2020.9223877.
- [4] M. Polivka, V. Hubata-Vacek, and M. Svanda, "Harmonic Balance/Full-Wave Analysis of Wearable Harmonic Transponder for IoT Applications," *IEEE Trans. Antennas Propag.*, vol. 70, no. 2, pp. 977–987, Feb. 2022, doi: 10.1109/TAP.2021.3111226.
- [5] Z. Ye, M. Yang, Y. Ren, C.-H. J. Hung, C.-T. M. Wu, and P.-Y. Chen, "Review on Recent Advances and Applications of Passive Harmonic RFID Systems," *IEEE J. Radio Freq. Identif.*, vol. 7, pp. 118–133, 2023, doi: 10.1109/JRFID.2023.3276310.
- [6] S. Khaledian, F. Farzami, B. Smida, and D. Erricolo, "Two-Way Backscatter Communication Tag Using a Reflection Amplifier," *IEEE Microw. Wirel. Compon. Lett.*, vol. 29, no. 6, pp. 421–423, Jun. 2019, doi: 10.1109/LMWC.2019.2912299.
- [7] X. Gu, R. Khazaka, and K. Wu, "Single-Ended Reconfigurable Wireless Power Harvesting and Harmonic Backscattering," in *IEEE Wireless Power Technol. Conf. Expo.*, Jun. 2023, doi: 10.1109/WPTCE56855.2023.10215912.
- [8] G. Paolini, A. Quddious, D. Chatzichristodoulou, D. Masotti, S. Nikolaou, and A. Costanzo, "An Energy-Autonomous SWIPT RFID Tag for Communication in the 2.4 GHz ISM Band," in *Atlantic Asia Pacific Radio Sci. Meet.*, May 2022, doi: 10.23919/AT-AP-RASC54737.2022.9814385.
- [9] Y. Qaragoz, S. Pollin, and D. Schreurs, "FDD for Low Power Backscattering in Batteryless Sensor Nodes," in *European Microw. Conf.*, Apr. 2022, pp. 753–756, doi: 10.23919/EuMC50147.2022.9784258.
- [10] —, "Frequency division duplex-multitone approach for backscatter aided swipt," in *Wireless Power Week*, 2022, pp. 213–217, doi: 10.1109/WPW54272.2022.9853856.
- [11] X. Sun, C. Liu, Y.-D. Chen, J. Jing, Z. He, and P. Wu, "Low-Power Wireless Uplink Utilizing Harmonic With an Integrated Rectifier-Transmitter," *IEEE Microw. Wirel. Compon. Lett.*, vol. 31, no. 2, pp. 200–203, Feb. 2021, doi: 10.1109/LMWC.2020.3043793.
- [12] P. Wu, S.-P. Gao, Y.-D. Chen, Z. H. Ren, P. Yu, and Y. Guo, "Harmonic-Based Integrated Rectifier-Transmitter for Uncompromised Harvesting and Low-Power Uplink," *IEEE Trans. Microw. Theory Tech.*, vol. 71, no. 2, pp. 870–880, Feb. 2023, doi: 10.1109/TMTT.2022.3200101.